Dynamic Performances of Multi-Renewable Energy Sources in a Microgrid During Islanding Operation

Piyadanai Pachanapan* and Suttichai Premrudeepreechacharn

***Abstract*—** *The dynamic performances of a microgrid system with multi-renewable energy sources, during the islanding condition, are presented in this paper. The test system consists of a small-scale hydro generator, photovoltaic (PV) system and battery energy storage system. In addition, the hydro generator is using the synchronous machine; while PV and battery systems are interfaced with the grid through power converters. The study aims to demonstrate the performance of islanding operation in a very light load condition, in which the total power generation from energy sources is extremely higher than the total demand. Three different control strategies are examined, which depending on technologies and functionalities of available energy sources in the system. The performance of each control strategy is simulated by using the transient simulation on DIgSILENT PowerFactory software. The simulation results illustrate that, in the islanding mode, the cooperated controls among hydro generator, PV and battery can deal with the changes of frequency and voltage during the islanding condition effectively. Additionally, the active power curtailment of hydro generator and PV system is required for this solution to restrict the power production, especially in the light load condition. Moreover, the Volt-Var supported by PV and battery systems can provide a fast voltage controllability during the islanding operation.*

***Keywords*— Distributed generation, islanding, microgrid, renewable energy sources, transient stability.**

1. INTRODUCTION

The growth of distributed generation (DG), both conventional and renewable energy sources, can improve power quality, reliability and security of supply to existed distribution networks, in the form of microgrid system. In addition, the microgrid system is an interconnected network of loads and DG units that can function whether they are connected to or separated from the main utility system [1]. The microgrid system can enhance power quality, such as voltage level improvement and loss reduction, to the network during the grid connecting mode, whilst it increases stability and reliability to the network in the islanding mode.

Islanding operation is an efficient control technique applied in the microgrid system when isolating from the main power system. The islanding condition is generally classified in two types: 1) Intentional or planed islanding which is a process of opening the circuit breaker/switch at the point of common coupling (PCC) to disconnect the microgrid and utility, and 2) Unintentional islanding which occurs due to a fault in the system and may lead to severe instability. During the islanding condition, there are significant changes in frequency and voltage. Therefore, the control strategy should secure the system frequency and voltage to stay within the statutory limits, as provided by some international standards such as IEEE 929-2000 or IEC 62116 [2].

There are many practical microgrid projects implemented by integrating with several renewable energy sources such as CERTS microgrid concept in North Amarica [3], the European Union MicroGrid project [4] and microgrid project in Sendai, Japan [5]. However, it was found that the small-scale hydro power plants are not involved in those projects. Most of microgrid systems are implemented based on converter-connected DG such as micro-turbine and photovoltaic (PV) system which can provide the fast control response. However, many rural areas, especially in Greater Mekong Subregion, have a high potential to include the small-scale hydro power plant to support the energy balancing process under the islanding condition. The frequency control response of hydro turbine governor control is possible to be included in the islanding operation, which the settling time is about 10-30 s, as demonstrated in [6]. Moreover, the experiment in [7] found that the use of hydro generator and PV system with power curtailment ability, when operating in the islanding mode, can improve the reliability performance to the microgrid system.

In this work, the test system consists of small hydro generator, PV and battery systems. The study aims to demonstrate the performances of islanded microgrid system in terms of frequency and voltage controls during the critical condition, that the aggregated generation from energy sources exceeds the local demand. Therefore, the active power curtailments from hydro generator and PV system are required. The various control strategies are applied which depends on the availability of control functions of hydro generator. The results from transient simulation studies based on practical load demand and PV generation will benefit the relevant person, such as the planning engineer, to

P. Pachanapan is with the Department of Electrical and Computer Engineering, Faculty of Engineering, Naresuen University, Phitsanulok 65000, Thailand.

S. Premrudeepreechacharn is with the Department of Electrical Engineering, Faculty of Engineering, Chiang Mai University, Chiang Mai 50200, Thailand.

*Corresponding author: P. Pachanapan; Phone: +66-55-96-4322; E-mail: piyadanip@nu.ac.th.

consider the suitable control solution, as well as the choice of controller's functions, which should be applied to operate the islanded microgrid system.

2. MICROGRID ARCHITECTURE AND ISLANDING FEATURES

The typical microgrid system adapted from [8] is showed in Fig. 1. The hierarchical control system architecture comprised the following two control levels: 1) device level at DG and energy storage units, and 2) microgrid central control (MGCC)

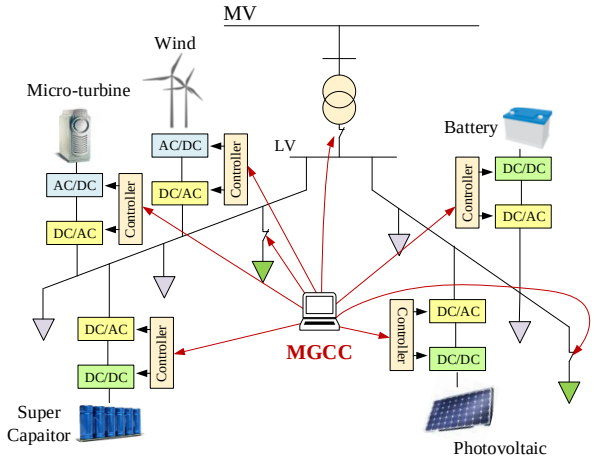

Fig.1. Typical microgrid architecture.

At the device level, DG and energy storage units try to generate power to the microgrid system that meet the grid requirement, such as system frequency and voltage level. There are two control strategies are commonly used in this level. One is the peer-to-peer control which each DG and energy storage unit has an equivalent status and no single component is critical for the microgrid operation. The other control strategy is the master-slave control, which the slave modules receive instructions from the master through communication channels. Additionally, a single DG or energy storage unit is selected as the master, to take the primary control action, while the other units are slaves. All controllable devices in both control schemes are also supervised by the MGCC.

The MGCC is the key level in the centralized control scheme. In this level, the central controller can command and exchange information with other controllable devices in the microgrid system via reliable communication links. The MGCC is used to coordinate power references of DG units and controllable loads, while each individual DG controller ensures that the set-point from the MGCC level is reached. In islanding mode, the MGCC will manage the power production of DG and energy storage units to match with the total load demand in the microgrid system. Thus, the voltage and frequency are regulated within the statutory limits. Moreover, the MGCC is able to disconnecting the uncontrollable DG and specific loads with the aim to maintain the reliability of the system.

To detect the loss of main condition, there are three main approaches for the islanding detection methods which are passive, active and commucation-based methods. The rate-of-change-of-frequency (ROCOF) and voltage vector shift (VVC) techniques, based on passive anti-islanding method, are famously used as the islanding detector of the microgrid system. The detail of these 2 techniques will be discussed as follows:

- The ROCOF relay is a local detection relay which does not require a communication system. The unbalance between local generation and load in the formed island resulting in the power mismatch that will cause the change of frequency (Δf). The ROCOF relay thus measures the voltage and estimates the rate of $\Delta f/\Delta t$ to investigate whether the loss of main condition occurs. Typical pickup values are set in a range of 0.1 to 5.0 Hz/s with the operation time between 0.1 s and 0.5 s [9].
- The VVS relay measures the voltage phase angle changes in consecutive cycles and compares the phase angle with the pre-set limit. Typically, the difference of phase angle should not be over 20^o in case of aggregated rating of energy sources is less than 500 kW [10].

To allow the microgrid supports the planned islanding operation, the following features are proposed for the MGCC [6]:

1) The islanding detection scheme should detect the loss of main condition as quick as possible. If the scheme fails to detect within the maximum detection time (i.e. 0.5 sec), the DG can be exploded with the risk of out of phase reclosing.
2) The microgrid system should have a radial structure. If it is a meshed/ring network, a normal open point should be located in between two selected feeders.
3) The availability of fast and reliable communication, such as fiber optic and global position system (GPS), is necessary for transferring data between MGCC and controllable devices.
4) Two different protection settings are employed for using in either grid connected and islanding modes.

3. CONTROL SYSTEMS OF RENEWABLE ENERGY SOURCES AND STORAGE SYSTEM

The control systems included in hydro, PV and battery systems are explained in this section. The hydro generator is based on synchronous machine and directly connecting to the network. On the other hand, PV and battery are DC sources which connect through the network via power electronic converter.

Small Hydro Generator

The small scale hydro generators are widely used in the rural areas. The power plant is commonly based on run-of-river design, which lacking of significant water storage, as seen in Fig. 2. The power output is decided by the water level which varies with rainfall. The power output of hydro turbine is given by, [1]

$$P = QH\eta\rho g \quad (1)$$

where P is output power (W), Q is flow rate (m^3/s), H is effective head (m), η is overall efficiency, ρ is density of water (1000 kg/m^3) and g is acceleration due to gravity.

Typically, there is no automatic power and voltage controllers in the small hydro power plant. This means that the hydro turbine will produce the power as much as possible to the microgrid system. Therefore, it may cause the surplus of power generation during islanding condition. To prevent this situation, the hydro generator will be disconnected or to be asked for the power curtailment if the active power controller is available.

The power production of hydro generator can be reduced by adjusting the position of penstock gate to dropping the water flow rate. This gate is adjusted by the servo actuator which is controlled by the governor. In addition, the governor will monitor the variation of system frequency or turbine speed, and then command the change of gate position. Fig. 3, demonstrates the simplified relationship between the basic elements of power generation process in a hydro power plant [11].

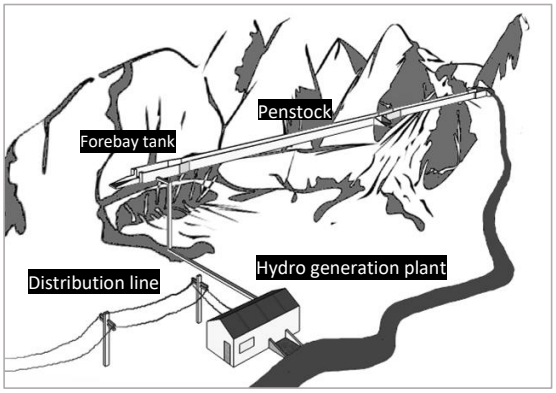

Fig.2. Run of river hydro power plant.

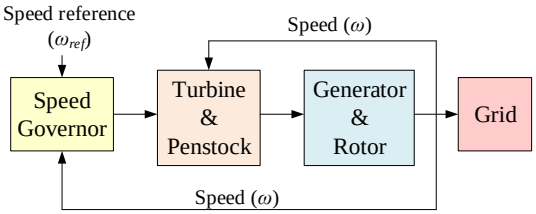

Fig.3. Functional block diagram of hydraulic power plant.

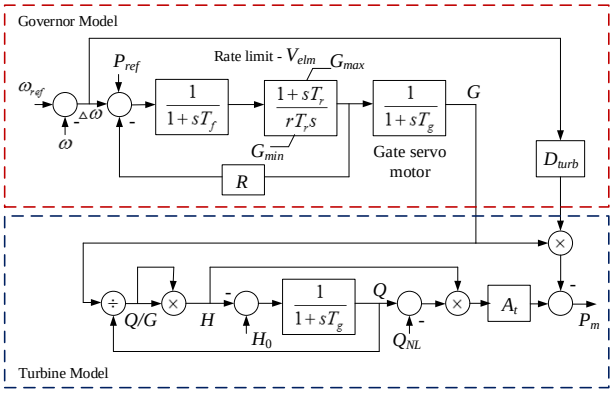

Fig.4. Hydro turbine governor model

The hydro turbine governor, based on HYGOV model in DIgSILENT *PowerFactory* software, is employed in this work, as illustrated in Fig. 4. This is typical model which consists of governor and non-linear hydro turbine models where the turbine efficiency and the hydraulic losses in penstock are taken into account. The turbine mechanical power (P_m) is proportional to the gate opening (G) and the turbine response time is depending on the water column time constant (T_w). The detail of hydro turbine governor's parameters is presented in Appendix. The values of governor control's parameters are selected based on the guideline in [12], while the typical values of turbine parameters are considered from [13].

Photovoltaic and Battery

The modern grid-tied PV and battery systems are typically based on voltage source converter (VSC) which consists of DC/DC converter cascading with DC/AC inverter, as illustrated in Fig. 5. The energy source-side VSC establishes the maximum power extraction function whilst the grid-side VSC performs the grid interface control. The active and reactive powers from grid-side converter can be controlled follows the supervision from the MGCC. Although both PV and battery systems have the same converter configuration, the PV is using uni-directional power converter while the bi-directional power converter is employed for the battery system.

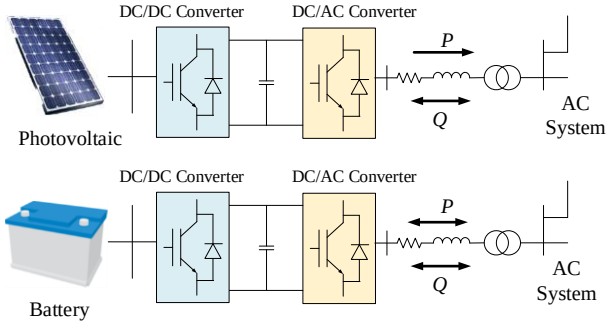

Fig.5. Configurations of grid-connected PV and battery.

During the normal condition, the active power from PV is variable depending on the weather conditions, such as temperature and solar irradiance. The PV system will operate in maximum power extraction mode, which is the energy captured from the sun according to the maximum power extraction algorithm. The PV system can operate in either *PQ* or *PV* mode [14]. In *PQ* mode, the reactive power of PV system is controlled at the fixed value or to be generated by the MGCC demand while the active power is still produced according to a maximum power extraction rule. Alternatively, the *PV* mode will arrow the PV system providing voltage control, to maintaining the AC voltage of inverter at a desired value.

In the case of battery system, the direction of active power of the battery is depending on it is charged or discharged. The battery sends active power to the microgrid system during the discharge mode, while, in the charge mode, the battery creates negative active power. The battery will be operated in charge or

discharge mode depending on the level of state-of-charge (SOC). If SOC is high, the battery has been filled with electricity and ready to discharge power the system. On the contrary, the battery should be recharged immediately when SOC is lower than the permission value. In term of reactive power produced by the battery, it is similar to the PV system which it is decided by the operating mode of the battery (*PQ* or *PV* mode) and the rated power of the grid-side converter. Moreover, the fast charging and discharging characteristics of the battery can be used to stabilize the power fluctuation from the PV generation, affected by the uncertain characteristic of sun intensity over the day.

In islanding mode, the grid-side inverter of either PV or battery system, especially the one chosen as the master device, will operate as a grid-forming inverter aiming to emulate the behavior of a synchronous machine by providing a reference for voltage and frequency when the microgrid system is isolated from the main grid [15]. If two or more converter based PV and energy storage units participate in grid frequency and voltage controls, the droop control methods are applied to share active and reactive power among those PV and battery units. The frequency-droop and voltage-droop characteristics can be written as;

$$P = -\frac{(f - f_0)}{K_P} \text{ and } Q = -\frac{(V - V_0)}{K_Q} \quad (2)$$

where P and Q are the active and reactive powers produced by the inverter, K_P and K_Q are the droop gains, f_0 and V_0 are the reference frequency and voltage.

The control scheme of grid-side VSC is developed based on the *dq* synchronous rotating reference frame which consist of consists of two cascaded control loops. The output of VSC is generated by using the pulse width modulation (PWM) technique. The inner control loop decouples the control for the real and imaginary current components [16]. This control method consists of two main classes of two dimensional frames, the *αβ*-frame and the *dq*-frame. Therefore, the two current components, i_d and i_q, are controlled independently, as shown in Fig. 6 (a). The reference values for the i_d and i_q controls are provided by the outter control loop, as demonstrated in Fig. 6 (b). The $i_{d,ref}$ is from the acitve power (*P*) or system frequency (*f*) controller on the *d*-axis, while the $i_{q,ref}$ is from the reactive power (*Q*) or bus voltage (*V*) controller on the *q*-axis. In both control loops, the error signals are compensated using PID and PI controllers.

Under the normal condition, PV system is in *PQ* mode where active and reactive powers are controlled to maintain the maximum power extraction and constant power factor, respectively. In addition, the *P* reference (P_{ref}) is defined from the energy source-side VSC, which is DC/DC converter. On the other hand, the PV system will change to control system frequncy and bus voltage after the islanding condition is detected. Therefore, the power production of PV system will be curtailed if the system frequency is higher than the reference value.

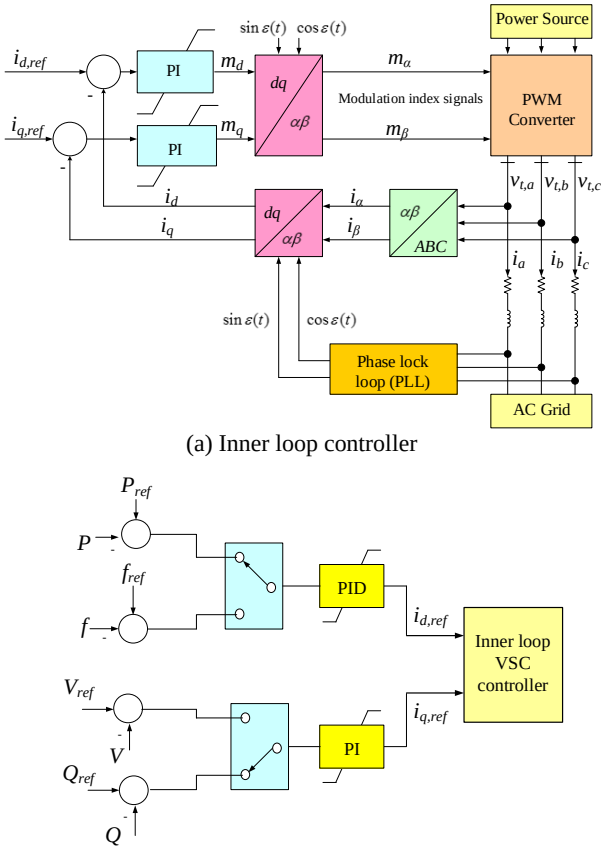

(a) Inner loop controller

(b) Outter loop controller

Fig.6. Grid-side VSC controller of PV and battery systems.

The controller diagram of battery energy storage system is the same as the PV system. In grid connecting mode, the battery system is in a standby mode which operating frequency and Volt-Var controls with the aim to stabilize the power fluctuation from the PV generation (called PV smoothing). However, the MGCC can command the value of P_{ref} to allow the battery supplying the active power during specific occasion, such as using the battery system in the load shifting machanism. When the loss of main occurs, the battery system will act as the master device by providing the reference voltage and frequence with the fast response. It is used as an frequency responsive device to maintain the stability of the islanded microgrid system. The surpassing energy can be absorbed by charging the battery until the SOC reaching the upper limit, whilst the battery will stop to dispatch further energy if the SOC is too low. Furthermore, the reactive power for supporting the voltage control can be shared among battery and PV systems, via the droop control method.

The PID and PI controllers' parameters of battery and PV systems are illustated in Appendix. The controllers' gains in battery and PV controllers obtained by fine tuning using Zeigler and Nicole method [17].

4. TEST SYSTEM AND CASE STUDY

The test system is 22 kV, 50 Hz distribution network which includes 100 kW hydro generator, 100 kW PV system and 100 kWh battery, as shown in Fig. 7.

Assuming the power output of hydro generator is constant for the whole day, while the PV generation varies following the availability of sunlight. Fig. 8, illustrates the power output characteristic of 100 kW PV system and daily aggregated demand. The MGCC will quickly detect the islanding condition; the switches M1, M2, S1 can be disconnected by the decision of MGCC to keep reliability and stability of microgrid system during the islanding condition. Furthermore, the MGCC is able to adjust the controller functions and power dispatches of battery and PV systems, for managing the islanded microgrid system to meet the Grid Code requirements.

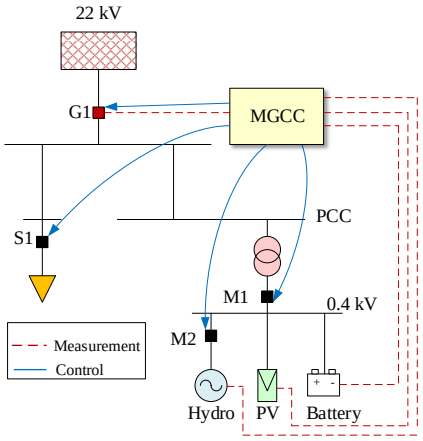

Fig.7. Test system

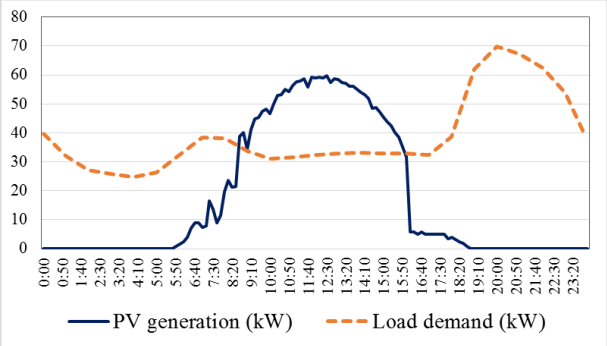

Fig.8. PV generation and load demand profiles.

During the grid-connecting condition, hydro generator and PV system dispatch active power according to the maximum extraction from their resources. There is no automatic voltage control for hydro generator. PV and battery system operate in *PQ* mode and standby mode, respectively. The battery stays in healthy condition, assuming that the level of SOC is in medium/high condition all the time.

When the MGCC receives the islanded command, the grid-side converters of energy sources are operated in the islanding mode. The MGCC will find the suitable control strategy to manage the microgrid system during the loss of main condition, which depending on the availability and control functions of energy sources in the system. If hydro generator and PV system cannot provide the frequency control, they may be forced to shut down by the MGCC. Then, the battery system is a controllable device to support voltage and frequency controls. On the other hand, hydro generator and PV system with power curtailment ability can be included in the instantaneous power balancing process, with a lesser amount of support from the battery.

This work aims to study the microgrid performance when operating the islanding management in the critical power mismatch situation, assuming as the aggregated power generation of renewable energy sources is much higher than the total load demand. At the first milliseconds of islanding transition, the battery system will suddenly acts as the master device and trying to absorb the excessive energy from both hydro generator and PV system. Then, the MGCC will send a command to PV system to operate in frequency and voltage control modes if the power curtailment function is available. The droop control methods are applied to share active and reactive powers among PV and battery systems. The MGCC will permit the hydro generator to stay connected if the turbine governor system is existing. The uncontrollable hydro generator may be included in the islanding operation if the output power is relatively low or the battery system has the room enough to engage with the surpassing power. Otherwise, the hydro generator needs to be disconnected from the microgrid system.

At initial condition, hydro generation supplies the constant power of 50 kW into the network, while the battery has the medium SOC at 50 %, which is ready to absorb and inject energy among energy sources in the microgrid system. The PV system operates in the *PQ* mode at unity power factor. Assuming the planed islanding is occurred at 11.00 a.m. when the load demand is the lowest (about 32 kW) while the PV system produces the highest power output at approximately 60 kW. Therefore, the total power production in the microgrid system will be 110 kW which the surplus power, about 78 kW, will flow backward to the main grid. The islanding condition is defined by tripping the load break switch G1, to separate the utility system and the microgrid system.

The performances of microgrid operation during islanding condition are simulated by using the transient analysis on DIgSILENT *PowerFactory* software. The timeframe for the simulation is 240 s. Assuming that the utility system is disconnected from the microgrid system at t = 10 s and then it is reconnected again at t = 110 s. After the islanding is detected, the MGCC will change to operate in the islanding mode within 0.3 s. During the loss of main grid, the MGCC will try to maximise the use of renewable energy sources with the fewer support from the storage energy devices. Additionally, the control strategy is decided based on the available of control functions of those energy sources.

After the microgrid system is re-connected to the main utility, the MGCC will be back to operate in the grid-connecting mode by stopping the support from the battery and re-operating the PV system back to the *PQ* mode. If the hydro generator is disconnecting during the islanding operation, it will be reconnected and to re-supplying the power again after the PV and battery systems are already back in the normal operation. The sequence of simulated events to examine the performance of islanding operation is shown in Table 1.

Table 1. Sequence of Simulated Events

Time (s)	Event
10	Switch G1 is opened
10.3	PV system is changed to frequency and voltage control mode
	The uncontrollable hydro generator is disconnected
110	The switch G1 is reclosed
111	The battery system is changed to the standby mode
120	The PV system is back to the *PQ* mode
125	The hydro generator is reconnected

In this study, the islanding management of microgrid system is exercised in three different control strategies, as followings;

Case 1: The hydro generator is not included in the islanding operation

Case 2: The hydro generator, without a turbine governor controller, is included in the islanding operation.

Case 3: The hydro generator, with a turbine governor controller, is included in the islanding operation.

5. SIMULATIONS AND RESULTS

The simulation results of microgrid system during the islanding transition is shown in Fig. 9 and Fig. 10. It is found that, after the switch G1 is opened, the transfer of surpassing powers, at about 78 kW, will be suddenly disappeared. In consequence, the power output of hydro generator will drop rapidly causing the rises of turbine speed and system frequency. At the same time, the battery system, which is the main frequency responsive device, will absorb the surplus energy from the PV system. The results show that the frequency continuously increase to 50.84 Hz with the rate of change = 2.8 Hz/s, before the MGCC operates in the islanding mode at t = 10.3 s. The voltage level at the PCC bus will reduce from 1.0 p.u. to 0.874 p.u. due to the loss of reactive power, which is about 19.6 kVar, supplied from the main grid. Moreover, the isolation from the main grid causes the shifting of PCC's voltage angle from 0.017^{o} to 19.88^{o}.

Fig. 11 to 13, show the voltage level, system frequency and power dispatched by each energy sources during islanding operation in different control strategies. The performance of each case study is discussed as follows.

Case 1

In this case, it is assumed that the PV and battery systems are sharing the supports of active and reactive powers during the islanding condition, while the MGCC will disconnected the small hydro generator by tripping the switch M2. After t = 10.3 s, The PV system starts to curtail the power output and also sharing the amount of reactive power with the battery system. Fig. 11, shows that the support from battery and PV system will take time about 5 s to recovery the voltage level back to the nominal value. There is some frequency fluctuations occur during the power balancing mechanism, and then the system frequency will become stable after 60 s. It is found that, during islanding operation, the active power of PV system is reduced from 60 kW to approximately 21 kW and the battery system is adding 11 kW to support the frequency control. Furthermore, PV and battery system inject the reactive power at 9.8 kVar/each to maintain the voltage level at around 1.0 p.u..

After switch G1 is re-connected, the MGCC will sending the command to the battery to stop injecting the power support. Then, 20 s later, the MGCC will change the PV system back to the *PQ* mode, which supplies the active power according to the maximum power extraction (60 kW) and the reactive power is back to zero (unity power factor). Finally, the MGCC will reconnect the switch M2 again, making the hydro generator to gradually increase the output power to reach 50 kW, which taking time about 100 s.

Case 2

The uncontrollable hydro generator, without governor and exciter controllers, is assumed to stay connected and then supplying the power output at 50 kW to the islanded mocrogrid system. The simulation results in Fig. 12, show the active power output of PV system is curtailed to zero, while the excessive power from the hydro generator, which is about 18 kW, is absorbed by the battery storage system. Moreover, the PV and battery systems will share the Volt-Var support which can keep the voltage level satisfyingly during the loss of main condition. After the grid-connecting is detected, the battery will be back to the standby condition, while the PV system will increase the generation back to 60 kW with the unity power factor.

Unlike the main utility, the small hydro power plant has the lacks of inertia and damping power. This cause some oscillations occurs to system frequency and voltage level during the islanding operation. In addition, these oscillations can be reduced by adding derivative control into the frequency controllers.

The battery system will be in the charge mode to absorb the surplus energy from the hydro generator in the islanded microgrid system, until the level of SOC reaching the upper limit. After the battery is charged fully, the hydro generator needs to be disconnected by opening the switch M1; battery and PV systems will take a responsibility to support frequency and voltage controls in the islanded microgrid system, as similar to the case 1. Moreover, the hydro generator can be included in the islanding operation again, if the SOC of battery is reduced to low/medium condition.

Case 3

In this case, the hydro generator with turbine-governor controller will be included in the power balancing process since the islanding has occurred. The speed of hydro turbine will be controlled during the loss of main condition, resulting in the smooth change of system frequency response, as demonstrated in Fig. 13. Moreover, the regulation from the turbine-governor will

decrease the output power of hydro generator gradually, from 50 kW to around 32 kW, to cover the local demand in the islanded microgrid system. As it known that the response of hydro turbine-governor is relatively slow, thus making it may be difficult to sustain islanding operation without the additional supports from PV and battery systems, especially at the beginning of islanding operation. It is found that the settling time of the turbine-governor control in this case is nearly 40 s. The frequency controllers of PV and battery systems will adjust their power outputs corresponding to the change of hydro generator output. Hence, active power outputs of PV and batters systems are reduced to zero after the frequency in the islanded microgrid system is regulated to meet the reference value (50 Hz), at $t \approx 20$ s.

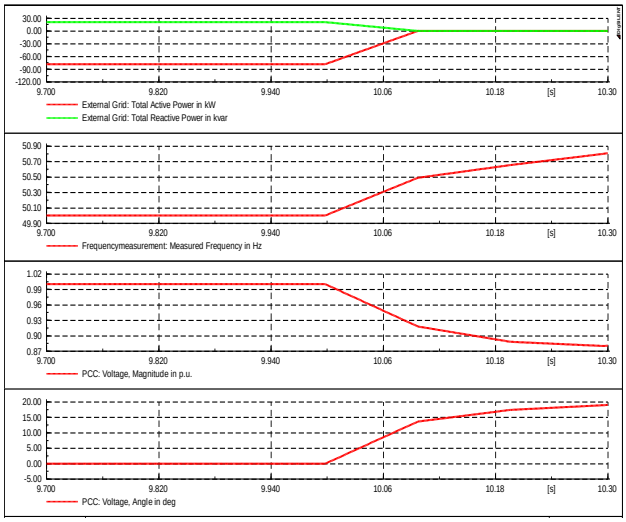

Fig.9. Powers at switch G1, frequency, voltage level and voltage angle during islanding transition.

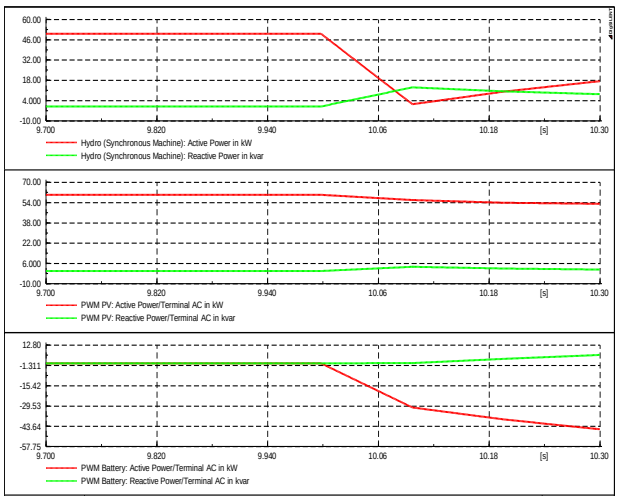

Fig.10. Outputs of hydro generator, battery and PV systems during islanding transition.

Both battery and PV systems will provide the additional Volt-Var support due to there is no the automatic voltage control installed in this hydro power plant. The results in Fig.13 show that the reactive power supported by hydro generator is about 13.6 kVar, while PV and battery will inject the extra reactive power, which is 3 kVar/each, making the voltage level to remain at 1.0 p.u.. Since the microgrid system is reconnected to the utility at t = 110 s, the hydro generator will slowly increase the power output to reach 50 kW again, at t ≈190 s, while the PV and battery systems will be resumed to operating in *PQ* mode, and standby mode, respectively. It can be seen that the changes of voltage and frequency in this control strategy is smoother when comparing to the two previous cases.

6. CONLUSION

From the simulation studies, it is found that the use of hydro generator with the turbine-governor controller, together with PV and battery systems, can deal with the changes of frequency and voltage in the islanded microgrid system effectively. If the load demand in the islanded microgrid system is relatively low, the power balancing process has been done by curtailing the active powers from the hydro generator and PV system, with fewer energy supported from the battery system. Moreover, the PV and battery system can support the voltage control with the fast response, by sharing the reactive powers among them.

It is possible to allow the uncontrollable hydro generator, which has no turbine-governor system, to include in the islanding operation. A surplus energy from the hydro generator will be absorbed by the battery system, while the power output of the PV system reduces to be zero. However, the lack of inertia and damping power of small hydro generation making the oscillations occur when the islanding operation has done under the very light load condition. In consequence, the islanded microgrid system may become instability if the damping control from the frequency responsive devices is not effective enough.

REFERENCES

[1] Jenkins, N.; Ekanayake, J.B. and Strbac, G. 2010. *Distributed Generation*. The Institution of Engineering and Technology.

[2] Singh, R. and Kirar, M. 2016. Transient stability analysis and improvement in microgrid. In *2016 International Conference on Electrical Power and Energy Systems (ICEPES)*, Bhopal, pp. 239-245.

[3] Alegria, E.; Brown, T.; Minear, E.and Lasseter, R.H. 2014. CERTS Microgrid Demonstration With Large-Scale Energy Storage and Renewable Generation," in *IEEE Transactions on Smart Grid*, vol. 5, no. 2, pp. 937-943.

[4] European Research Project More MicroGrids. [Online]. Retrieved October 16th, 2017 from the world wide web: http://www.microgrids.eu/default.php

[5] Sendai Microgrid. [Online]. Retrieved October 16th, 2017 from the world wide web: http://microgrid-symposiums.org/microgrid-examples-and-demonstrations/sendai-microgrid/

[6] Mohamad, H.; Dahlan, N.N.; Bakar, A.H.A.; Ping, H.W. and Mokhlis, H. "Islanding control strategy for a distribution network," *2013 IEEE 7th International*

Power Engineering and Optimization Conference (PEOCO), Langkawi, 2013, pp. 472-477.

[7] Pachanapan, P. 2018. Islanding Management of Microgrid with Multi-renewable Energy Sources. In *GMSARN International Journal*, vol. 12, no. 2, June 2018, pp. 47-55.

[8] Li, S.; Proano, J. and Zhang, D. 2012. Microgrid power flow study in grid-connected and islanding modes under different converter control strategies. In *2012 IEEE Power and Energy Society General Meeting*, San Diego, CA.

[9] Chan, C.Y.; Lau, T.K.Y and Ng, S.K.K. 2015. An impact study of ROCOF relays for islanding detection. In *10th International Conference on Advances in Power System Control, Operation & Management (APSCOM 2015)*, Hong Kong, pp. 1-6.

[10] (2013). IEEE Standard for Interconnecting Distributed Resources with Electric Power Systems. IEEE Std 1547-2003, pp. 1-28.

[11] Naghizadeh, R.A.; Jazebi, S. and Vahidi, B. 2012. Modeling Hydro Power Plants and Tuning Hydro Governors as an Educational Guideline. In *International Review on Modelling and Simulations*, vol. 5, no. 4, August 2012.

[12] TURBINE-GOVERNOR MODELS: Standard Dynamic Turbine-Governor Systems in NEPLAN Power System Analysis Tool. NEPLAN AG pp. 91.

[13] Kundur, P. 1994. *Power System Stability and Control*, McGraw-Hill, New York.

[14] Li, S.; Proano, J. and Zhang, D. 2012. Microgrid power flow study in grid-connected and islanding modes under different converter control strategies. In *2012 IEEE Power and Energy Society General Meeting*, San Diego, CA.

[15] Katiraei, F.; Iravani, R.; Hatziargyriou, N. and Dimeas, A. 2008. Microgrids management. In *IEEE Power and Energy Magazine*, May-June. vol. 6, no. 3, pp. 54.

[16] Yazdani, A. and Iravani, R. 2010. *Voltage-Sourced Converters in Power Systems*, 1st ed.: Wiley, chapter 8.

[17] Sharma, R.; Singh, A. and Jha, A.N. 2014. Performance evaluation of tuned PI controller for power quality enhancement for linear and non-linear loads, In *Recent Advances and Innovations in Engineering (ICRAIE), 2014*, Jaipur, India.

APPENDIX

Table 2. Parameters of Hydro Turbine-Governor

Parameter	Description	Value
H	Inertia time constant [s]	4.5
D	Mechanical damping [pu]	0.1
r	Temporary droop [pu]	0.1
R	Permanent droop [pu	0.04
T_r	Governor time constant [s]	10
T_f	Filter time constant [s]	0.1
T_g	Servo time constant [s]	0.5
T_w	Water starting time [s]	1.0
A_t	Turbine gine [s]	1.0
D_{turb}	Frictional losses factor [pu]	0.01
Q_{NL}	No load flow [pu]	0.01
G_{max}	Maximum gate limit [pu]	1.0
G_{min}	Minimum gate limit [pu]	0
V_{elm}	Gate velocity limit [pu]	0.15

Table 3. Controllers' Gains of PV and Battery Systems

Controllers	Gain parameters	
i_d controller	$K_P = 0.4$	$T_I = 0.01$
i_q controller	$K_P = 0.4$	$T_I = 0.01$
P/f controller	$K_P = 0.2$	$T_I = 0.05$; $K_D = 30$
Q/V controller	$K_P = 0.2$	$T_I = 0.3$

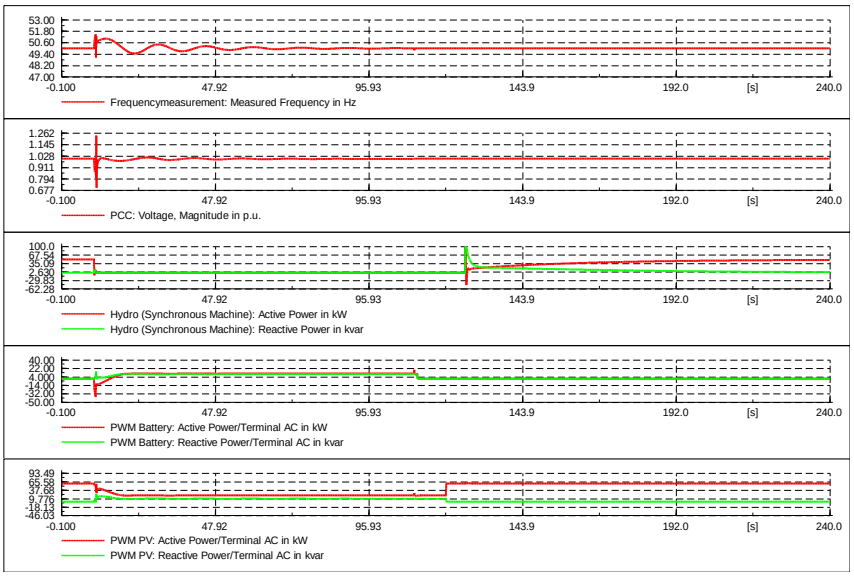

Fig.11. Simulation results of Case 1 (System frequency, voltage level, outputs of hydro generator, battery and PV systems).

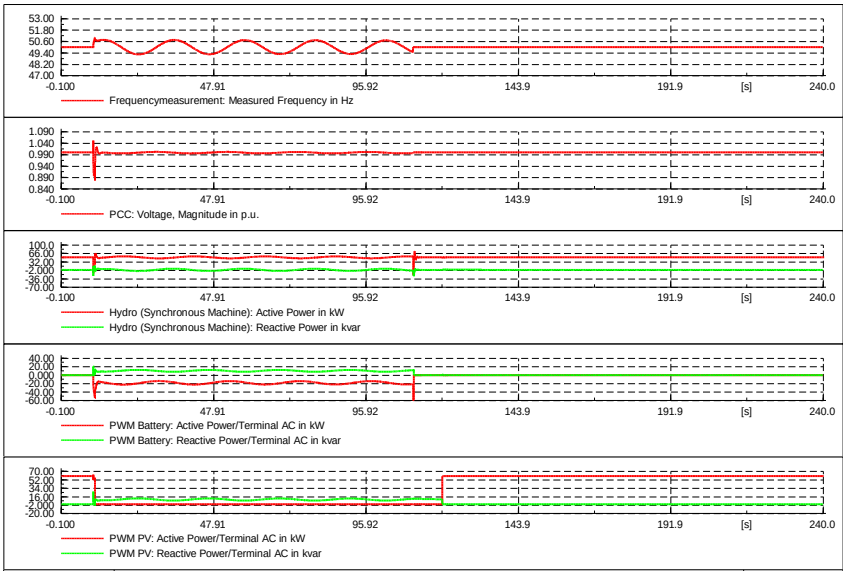

Fig.12. Simulation results of Case 2 (System frequency, voltage level, outputs of hydro generator, battery and PV systems).

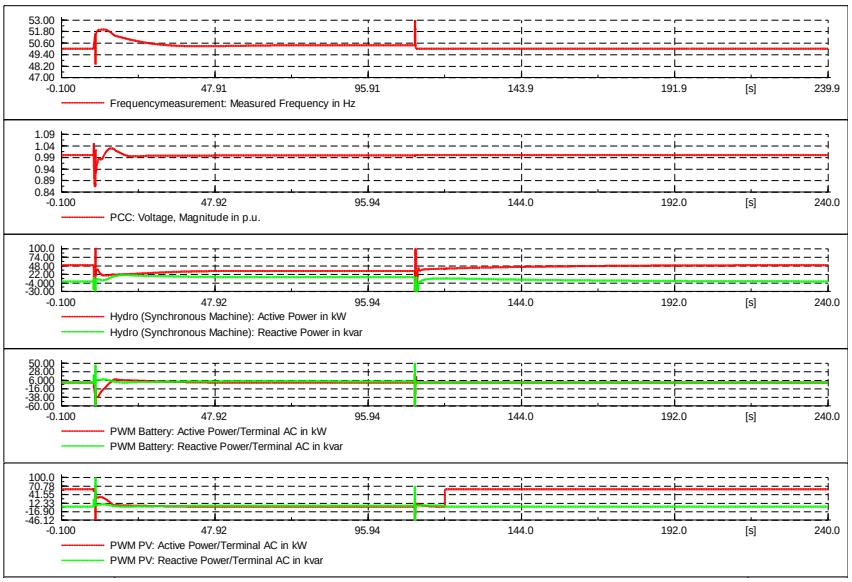

Fig.13. Simulation results of Case 3 (System frequency, voltage level, outputs of hydro generator, battery and PV systems).